Published OnlineFirst July 27, 2010; DOI: 10.1158/1535-7163.MCT-10-0051

Dihydroartemisinin Induces Apoptosis by a Bak-Dependent Intrinsic Pathway

René Handrick[1,4], Teona Ontikatze[1], Kerstin-Daniela Bauer[3], Florian Freier[3], Amelie Rübel[3], Jan Dürig[2], Claus Belka[3,5], and Verena Jendrossek[1,3]

Abstract

The sesquiterpene lactone dihydroartemisinin (DHA), a semisynthetic derivative of the herbal antimalaria drug artemisinin, is cytotoxic to human tumor cells. Treatment of Jurkat T-lymphoma cells with DHA induced a breakdown of the mitochondrial transmembrane potential, release of cytochrome *c*, activation of caspases, and DNA fragmentation indicative of apoptosis induction. Although the absence of FADD or caspase-8 did not alter apoptosis rates in Jurkat cells, overexpression of dominant-negative caspase-9 or of antiapoptotic Bcl-xL or Bcl-2 largely decreased the cytotoxicity of DHA, demonstrating a role of the intrinsic death pathway. The proapoptotic Bcl-2 effector protein Bak and the Bcl-2 homology domain 3–only protein NOXA turned out to be important mediators of DHA-induced apoptosis in Jurkat cells. DHA treatment triggered the expression of NOXA and the activation of Bak. Furthermore, DHA-induced apoptosis was completely abrogated by loss of Bak and largely reduced in cells with siRNA-mediated downregulation of Bak or NOXA. Proapoptotic signaling of DHA also involved the formation of reactive oxygen species and membrane oxidation. Pretreatment with the lipophilic radical scavenger vitamin E or the hydrophilic radical scavengers glutathione and *N*-acetylcysteine reduced DHA-induced membrane oxidation and apoptosis, respectively. Oxidative changes also occurred in cells with disruption of the mitochondrial death pathway, suggesting a role of reactive oxygen species and oxidative membrane changes in death signaling upstream of the mitochondria. Interestingly, DHA increased the cytotoxic action of ionizing radiation and of the death receptor agonist tumor necrosis factor-related apoptosis-inducing ligand in Jurkat cells, suggesting a potential benefit of DHA in combined treatment strategies. *Mol Cancer Ther; 9(9); 2497–510. ©2010 AACR.*

Introduction

Resistance of tumor cells to apoptosis is a major obstacle in anticancer treatment. Therefore, current researches focus on the development of innovative compounds that increase the death of therapy-resistant tumor cells. Artemisinin (Coartem/Riamed) from *Artemisia annua* L. is a natural endoperoxide that effectively forms radicals and reactive oxygen species (ROS; Supplementary Fig. S1; ref. 1). Artemisinin and its semisynthetic derivatives are potent antimalarial drugs acting against the chloroquine-resistant pathogen *Plasmodium falciparum* (2). The drugs are metabolized to the highly reactive hemiacetal dihydroarthemisinin (DHA), the active metabolite of this drug class, *in vivo* (Supplementary Fig. S1; ref. 2). Activation of the endoperoxide bridge is a prerequisite for the generation of ROS and of carbon-centered radicals. Subsequent alkylation of essential parasite proteins such as the Ca^{2+} ATPase SERCA (3), in concert with lipid peroxidation of vacuole membranes, triggers autodigestion of the parasite (4). Heme and heme iron seem to be important for oxidation and to determine the selective toxicity to intra-erythrocytary parasites (trophozoides, shizontes; ref. 5).

ROS and carbon-centered radicals also contribute to the potent cytotoxic effects of artemisinin and derivatives on tumor cell lines *in vitro* (4–7). Cytotoxic efficacy of these agents was increased by the addition of iron(II) salts alone and in combination with transferrin *in vitro* (8) and *in vivo* (9). The enhanced uptake of iron by tumor cells has been proposed to selectively increase drug-induced cytotoxicity on tumor cells compared with normal tissue cells (10). Recent reports show a role of apoptosis in the antineoplastic action of artemisinin and derivatives (11–13). However, the molecular details

Authors' Affiliations: [1]Institute of Cell Biology (Cancer Research), Department of Molecular Cell Biology, Medical School, University of Duisburg-Essen; [2]Department of Hematology, University Hospital Essen, Essen, Germany; [3]Department of Radiation Oncology, Experimental Radiation Oncology Group, University of Tübingen, Tübingen, Germany; [4]Institute of Pharmaceutical Biotechnology, University of Applied Sciences, Biberach, Germany; and [5]Department of Radiation Oncology, Ludwig-Maximilian University Munich, Munich, Germany

Note: Supplementary material for this article is available at Molecular Cancer Therapeutics Online (http://mct.aacrjournals.org/).

Corresponding Author: Verena Jendrossek, Institute of Cell Biology, University of Duisburg Essen, Virchowstr. 173, Essen, 45122, Germany. Phone: 49-201-7233380; Fax: 49-201-7235904. E-mail: verena.jendrossek@uni-due.de

doi: 10.1158/1535-7163.MCT-10-0051

Published OnlineFirst July 27, 2010; DOI: 10.1158/1535-7163.MCT-10-0051

of the proapoptotic action of these drugs in tumor cells, particularly the role of the extrinsic and the intrinsic apoptosis pathway, are still controversial (14, 15).

The extrinsic apoptosis pathway is initiated by binding of specific death receptor ligands [e.g., CD95 or tumor necrosis factor-α apoptosis-inducing ligand (TRAIL)] to their respective membrane receptors. Activation of the death receptors results in receptor multimerization and the recruitment of the adaptor protein Fas-associated death domain (FADD) and an initiator caspase, mainly procaspase-8, to build the death-inducing signaling complex. Autoproteolytic activation of the initiator caspase-8 in this complex with subsequent caspase-8–mediated proteolytic activation of the effector caspase cascade (16) results in the cleavage of a plethora of downstream caspase targets [e.g., DNA repair enzymes such as poly(ADP-ribose) polymerase (PARP)] and finally cell death. In contrast, cellular stress triggers the activation of the intrinsic, mitochondria-dependent apoptosis pathway. Activation of proapoptotic Bcl-2 proteins induces a breakdown of the mitochondrial membrane potential and the release of cytochrome *c* and further proapoptotic proteins such as second mitochondria-derived activator of caspases, apoptosis-inducing factor (AIF), and EndoG into the cytosol. Cytosolic cytochrome *c* binds to Apaf-1 in a dATP-dependent manner and recruits the initiator caspase procaspase-9 to form the apoptosome. Activation of caspase-9 then triggers the downstream effector caspase cascade, resulting in apoptosis. Proapoptotic and antiapoptotic members of the Bcl-2 family of proteins tightly control the activation of the intrinsic apoptosis pathway by regulating mitochondrial homeostasis and permeability (17). Activation of the proapoptotic multidomain proteins Bax or Bak or both is absolutely required for the initiation of the intrinsic apoptotic pathway, whereas antiapoptotic members like Bcl-2, Bcl-xL, and Mcl-1 prevent apoptosis initiation by binding to and inactivating their proapoptotic counterparts. The proapoptotic Bcl-2 homology domain 3 (BH-3)–only proteins (e.g., Bid, Bim Bad, PUMA, and NOXA) have only the BH-3 domain in common and constitute sensors of cellular stress. Two distinct but not mutually exclusive models for the activation of proapoptotic Bax and Bak have recently been proposed. According to the "displacement model," activation and subsequent binding of BH-3–only proteins to Bcl-2, Bcl-xL, Bcl-w, Mcl-1, or A1 displace Bax and Bak from these antiapoptotic proteins to allow their proapoptotic action. In contrast, in the so-called direct activation model, the BH-3–only proteins tBid, Bim, or Puma are assumed to directly activate proapoptotic Bax or Bak, whereas the sensitizer BH-3–only proteins Bad, Bik, Bmf, Hrk, and NOXA are needed for the release of tBid, Bim, and Puma from the antiapoptotic Bcl-2 proteins, resulting in the activation of Bax and Bak. Each BH-3–only protein is activated on specific stress conditions and displays favored interactions with specific antiapoptotic family members (17, 18).

The aim of the present study is to dissect the details of apoptosis signaling induced by the artemisinin-derivative DHA and to provide a molecular basis for the use of DHA in combined treatment strategies. Our study identified the Bcl-2 proteins Bak and NOXA as key mediators of DHA-induced apoptosis in Jurkat cells. Moreover, our data suggest a role of ROS formation and membrane oxidation for DHA-induced activation of the intrinsic apoptosis pathway. These oxidation events may contribute to the observed increase in the efficacy of TRAIL or radiotherapy in combination with DHA.

Materials and Methods

Chemicals and drugs

Dihydroartemisinin [DHA; (3,5,6,8,9,10,12R,12*aR*)-decahydro-3,6,9-trimethyl-3,12-epoxy-12*H*-pyrano[4,3-*j*]-1,2-benzodioxepin-10-ol, $C_{15}H_{24}O_5$] was dissolved to a final concentration of 40 mmol/L in ethanol. Hoechst 33342 (1.5 mmol/L, Calbiochem) and propidium iodide (PI, 5 mg/mL) were dissolved in water. zVAD-fmk was obtained from Bachem Distribution Services GmbH. Recombinant human TRAIL was from R&D Systems. Carbonylcyanide-*m*-chloro-phenylhydrazone was from Sigma-Aldrich. Tetramethylrhodamine-ethylester-perchlorate (TMRE) was from Molecular Probes (MoBiTec).

Antibodies specific for full-length and cleaved PARP (Asp214), caspase-3, Bak, AIF, α/β-tubulin (Cell Signaling), caspase-9, catalase, Bcl-xL, BakNT (Biomol/Upstate), FADD and Bax (BD Transduction Labs), Endo G (ProSci, BioCat), β-actin (Sigma-Aldrich), and caspase-8 (Bio-Check), and horseradish peroxidase–conjugated secondary antibodies (Amersham Biosciences), were used. A conformation-specific mouse monoclonal antibody (TC100/AM03, Merck/Calbiochem) was used for the detection of activated Bak.

If not otherwise specified, chemicals were purchased from Sigma-Aldrich.

Cell lines and culture

Jurkat E6.1 and Bak-positive JCaM1.6 (Bax-negative/Bak-positive subclone; subsequently named JCaM Bak positive) T-lymphoma cells were obtained from the American Type Culture Collection in 2004. The Bax/Bak double-negative JCaM1.6 subclone (subsequently named JCaM Bak negative) was used as described recently (19). Jurkat A3 control cells as well as the caspase-8 and FADD-negative Jurkat A3 cells were a gift from P. Juo and J. Blenis. The caspase-9 dominant-negative (DN) construct was kindly provided by E. Alnemri. Jurkat vector cells (Jurkat vector) as well as clones with cytomegalovirus-dependent constitutive expression of Bcl-xL (Jurkat Bcl-xL) and of wild-type Bcl-2 (Jurkat Bcl-2) were used as previously described (20). HCT116 wild-type and Bax-deficient HCT116 cells from B. Vogelstein (Johns Hopkins, Baltimore, MD) were kindly provided by P.T. Daniel (Department of Hematology, Oncology and Tumor Immunology, University Medical Center

Published OnlineFirst July 27, 2010; DOI: 10.1158/1535-7163.MCT-10-0051

Charité, Campus Berlin-Buch, Humboldt University, Berlin, Germany) in 2004 (21).

The phenotype of the distinct cell lines was proven before and during the acquisition of the experimental data using Western blot analyses with antibodies specific for Bax or Bak, caspase-8 and FADD, or caspase-9, respectively. No further authentication was done.

Cells were grown in RPMI 1640 supplemented with 10% (v/v) fetal calf serum (FCS; Gibco Life Technologies) and maintained in a humidified incubator at 37°C and 5% CO_2. Cell number and viability was quantified by counting cells stained with trypan blue at ×20 magnification (inverse microscope, Hund) using a Neubauer counting chamber.

Primary cells from patients with chronic lymphocytic leukemia

Blood samples from patients with chronic B-lymphocytic leukemia (B-CLL) were obtained from the Department of Hematology, University Hospital Essen, Essen, Germany. Informed consent was obtained from all patients before receiving the samples. Patients had been untreated (five of six), or chemotherapy had been completed 8 years earlier (one of six). All CLL cases had previously been analyzed for the presence of prognostically relevant cytogenetic abnormalities (Supplementary Table S1). The percentage of $CD19^+CD5^+$ leukemic cells as defined by flow cytometry exceeded 80% in each of the samples. Peripheral blood mononuclear cells were isolated by Ficoll-Paque density centrifugation, subjected to erythrocyte lysis [155 mmol/L sodium chloride, 10 mmol/L $KHCO_3$, 0.1 mmol/L EDTA (pH 7.4)], and subsequently plated in conditioned medium of HS5 bone marrow stromal cells collected after 48 hours of culture in DMEM medium supplemented with 10% FCS, 2 mmol/L glutamine, penicillin, and streptomycin. Cells were treated 2 hours after plating and cultured for further 24 or 48 hours.

Drug treatment and irradiation

Cells were treated for up to 24 hours with 2.5 to 40 μmol/L DHA. Treatments with etoposide (20–25 μmol/L), TRAIL (1–10 ng/mL), or 250 μmol/L H_2O_2 were used as controls. All experiments were done with a solvent control (0.1% ethanol). Irradiation was done at room temperature with 6 MV photons from a linear accelerator (Precise Treatment System, Elekta) at a dose rate of 4 to 5.8 Gy/min. For combined treatment, DHA was added 10 minutes before irradiation or 10 minutes after the addition of TRAIL, respectively. Pretreatment with the pan-caspase inhibitor zVAD-fmk was done 30 minutes before further treatment.

Characterization of cell death

Cell death was quantified by flow cytometry (FACSCalibur, Becton Dickinson) of FITC-Annexin V/PI–stained cells. Cells were incubated for 15 minutes in the dark with FITC-coupled Annexin V and PI in binding buffer (pH 7.4, 1.4 mol/L NaCl, 25 mmol/L $CaCl_2$), diluted with binding buffer, and measured within 1 hour (Fl-1 and Fl-2; BD Transduction Labs).

Changes in nuclear morphology were analyzed by fluorescence microscopy (Zeiss Axiovert 200, Carl Zeiss; G365/FT395/LP420 filter set) on cell staining with 1.5 μmol/L Hoechst 33342 and 2.5 μg/mL PI (×40 magnification). Apoptotic and necrotic cells were quantified by counting the relative amount of fragmented blue or red nuclei (early or late apoptosis) and nonfragmented red nuclei (necrosis).

For quantification of DNA fragmentation, cells were incubated for 60 minutes at room temperature in the dark in 0.1% (w/v) sodium citrate with 50 μg/mL PI and 0.05% (v/v) Triton X-100 and subsequently subjected to flow cytometry (FL-2 log).

Characteristic breakdown of the mitochondrial transmembrane potential ($\Delta\psi_m$) was analyzed by flow cytometry using the $\Delta\psi_m$-specific stain TMRE (FL-2) as described elsewhere (19).

Caspase activation was determined by Western blot analysis using antibodies against the active cleavage fragments of caspase-8, caspase-9, and caspase-3, and against the caspase-3 substrate PARP.

Western blot analysis

Cells were lysed for 10 minutes at 99°C in 62.5 mmol/L Tris-HCl (pH 6.8), 2% (w/v) SDS, 10% (v/v) glycerol, 50 mmol/L DTT, and 0.01% (w/v) bromphenol blue. Proteins were separated by 12.5% SDS-PAGE and blotted onto polyvinylidene difluoride membranes (Roth). After blocking with 5% (w/v) nonfat dry milk (or 5% bovine serum albumin for Bak detection), membranes were incubated at 4°C overnight with the respective primary antibody (1:1,000; 1:20,000 for β-actin). After washing, the membranes were incubated for 1 hour at room temperature with the secondary antibody (anti–IgG-horseradish peroxidase 1:2,000, Amersham Biosciences), washed again, and developed using enhanced chemoluminescence staining (ECL Western blotting analysis system, Amersham Biosciences). Equal protein loading was confirmed by β-actin/tubulin detection and Coomassie staining. Ratiometric densitometry analysis of protein expression compared with the loading controls was done using Photoshop/ImageJ.

Activation of Bak

PBS-washed cells were fixed for 20 minutes on ice in 2.5% (w/v) paraformaldehyde/PBS. Fixed cells were washed [1% (v/v) FCS in PBS], made permeable for 5 minutes at room temperature in 1% (v/v) FCS/PBS with 50 μg/mL digitonin, labeled for 45 minutes with an activation-specific anti-Bak IgG (or isotype control), washed, and then stained for 45 minutes with Alexa Fluor488–conjugated goat anti-mouse antibody (Molecular Probes, MoBiTec). Cells were washed and suspended in blocking buffer for subsequent flow cytometry (FL-1).

Published OnlineFirst July 27, 2010; DOI: 10.1158/1535-7163.MCT-10-0051

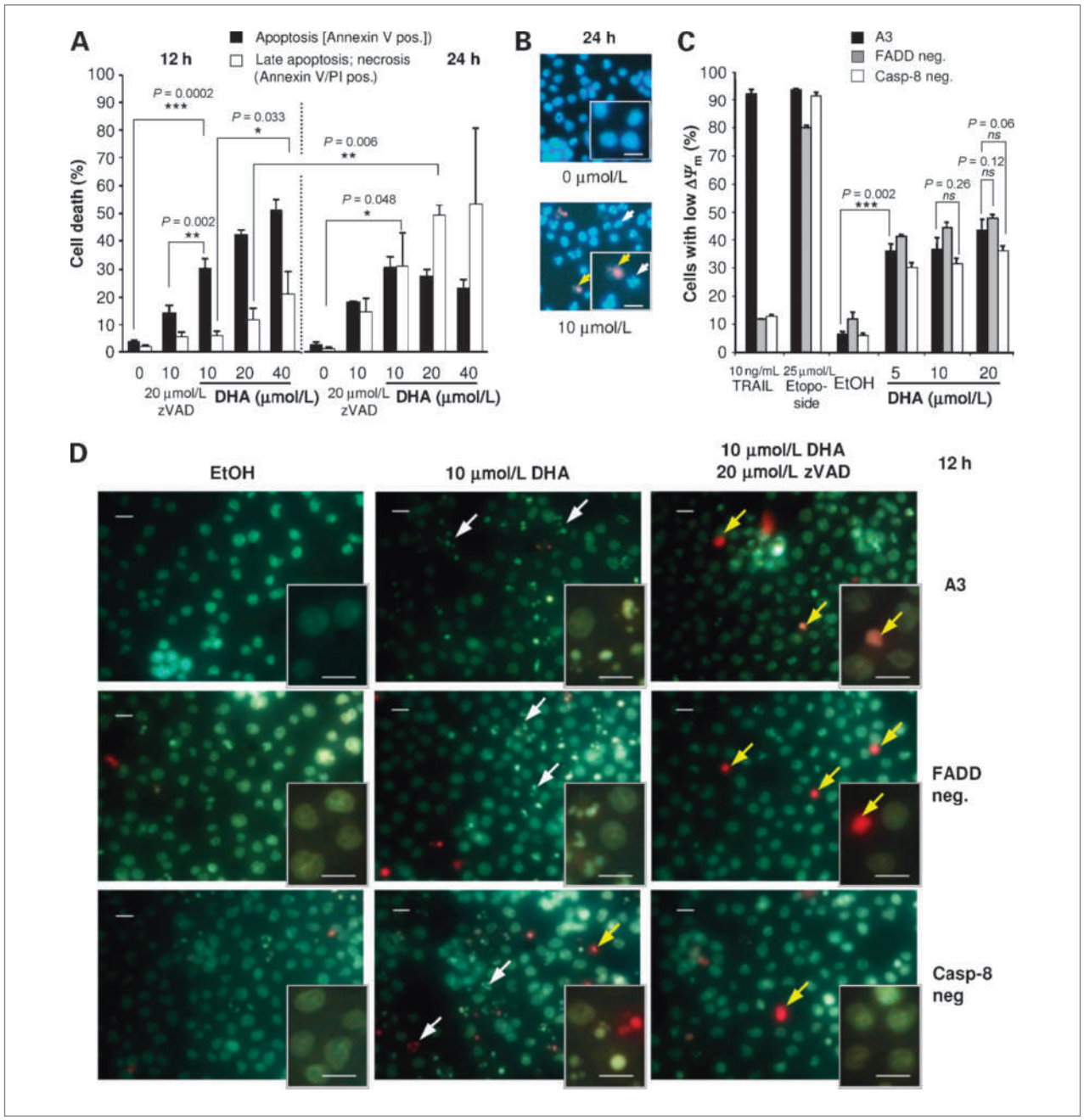

Figure 1. DHA induces apoptosis independently from caspase-8 and FADD in Jurkat T-lymphoma cells. Jurkat E6.1 (A and B), as well as wild-type, FADD-negative, or caspase-8–negative Jurkat A3 cells (C and D) were treated for 12 or 24 h with 0 to 40 µmol/L DHA as indicated. Prior incubation for 30 min with 20 µmol/L zVAD was used as control for caspase-dependent events. Treatment with etoposide (25 µmol/L) and TRAIL (10 ng/mL) was used to control the integrity of the intrinsic pathway and disruption of the extrinsic apoptosis pathway, respectively. Induction of apoptosis was measured 12 and/or 24 h after treatment. A and B, DHA treatment induced a time- and concentration-dependent breakdown of the phosphatidylserine asymmetry at the cytoplasmic membrane and apoptosis. A, breakdown of the phosphatidylserine asymmetry in the cytoplasmic membrane was determined by flow cytometry on loading of the cells with FITC-labeled Annexin V/PI in a Ca^{2+}-containing buffer. Data are means ± SD (n = 3; ANOVA: *, $P < 0.05$; **, $P < 0.01$; ***, $P < 0.001$; and-two tailed P values of paired t tests). B, nuclear morphology was analyzed by fluorescence microscopy of cells stained with Hoechst 33342/PI 24 h after treatment. Data are representative microscopic pictures (magnification 20-fold; inset, 40-fold; white arrowheads, apoptotic nuclei; yellow arrowheads, necrotic nuclei; white scale bars, 10 µm). C, DHA induced a concentration-dependent breakdown of $\Delta\psi_m$ and apoptosis with almost similar potency in caspase-8– and FADD-negative Jurkat A3 cells and in A3 wild-type cells. $\Delta\psi_m$ was determined 24 h after DHA treatment by flow cytometry on loading of the cells with the potential sensitive dye TMRE (means ± SD.; n = 3; ANOVA: *, $P < 0.05$; **, $P < 0.01$; ***, $P < 0.001$; and two tailed P values of paired t tests). D, DHA treatment induces apoptosis in Jurkat A3, caspase-8–negative, and FADD-negative Jurkat cells (white arrows). Inhibition of apoptosis by zVAD triggers necrotic cell death (yellow arrows). Nuclear morphology was analyzed by fluorescence microscopy of Hoechst 33342/PI–stained cells. Data are representative pictures from one of three independent experiments. EtOH, ethanol.

Published OnlineFirst July 27, 2010; DOI: 10.1158/1535-7163.MCT-10-0051

siRNA transfection

Exponentially growing cells were suspended in RPMI 1640 without phenol red. Anti-Bak ON-TARGET SMART pools, anti-NOXA ON-TARGET SMART pools, or nontargeting siRNA (80 μmol/L in H_2O, Dharmacon) were added to the cells at a final concentration of 0.5 to 1 μmol/L. Electroporation was done in a 4-mm cuvette (Bio-Rad Laboratories) in an EPI2500 electroporator (Fischer) at 400 V/10 ms. Cells were immediately suspended in 6 mL prewarmed medium and cultured as described above. Cell viability was determined by flow cytometry of PI-stained cells. Transfection efficiency was determined by flow cytometry of cells transfected with 400 nmol/L green fluorescence siRNA (siGLO, Dharmacon). Downregulation of the target protein was verified by densitometric analysis of Western blots 48 hours posttransfection.

ROS measurement

Cells were stained for 15 minutes with 5 μmol/L of the H_2O_2-sensitive dye dichlorofluorescein diacetate (DCFDA) or the superoxide-sensitive dye dihydroethidium (Molecular Probes, MoBiTec) at 37°C in the dark, washed with PBS, and analyzed by flow cytometry (DCFDA: green fluorescence FL-1; dihydroethidium: red fluorescence FL-2).

For detection of membrane-specific ROS, cells were loaded for 30 minutes at 37°C with 100 μL C11-Bodipy$^{581/591}$ (FC 1 μmol/L; Molecular Probes, MoBiTec), collected by centrifugation, and suspended in PBS. Oxidation-induced decrease in red fluorescence and increase in green fluorescence were measured by flow cytometry (FL-2 and FL-1).

Statistics

Data were analyzed by repeated-measures ANOVA using parametric methods and Bonferroni multiple comparison posttest with P values <0.05. Two-tailed P value paired t tests were run where appropriate. Analysis was done using InStat3 and Prism5 software (GraphPad, Inc.). To test additive or synergistic effects of DHA in combination with TRAIL or irradiation, isobologram analysis according to Berenbaum (22) was done.

Results

DHA induces apoptosis in Jurkat T-lymphoma cells

We first characterized the cytotoxic action of DHA (0–40 μmol/L) in apoptosis-competent Jurkat cells. DHA treatment potently induced apoptosis of Jurkat E6.1 cells. This was shown by a time- and concentration-dependent increase in FITC-Annexin–positive/PI-negative early apoptotic cells and FITC-Annexin/PI double-positive late apoptotic cells (Fig. 1A), and the appearance of cells with collapsed mitochondrial transmembrane potential (low $\Delta\Psi_m$) or hypodiploid nuclei (not shown). Staining with Hoechst 33342/PI confirmed apoptosis-related chromatin condensation and nuclear fragmentation in response to DHA treatment (Fig. 1B). The strong increase of FITC-Annexin/PI double-positive cells 24 hours after treatment indicated a shift to late apoptosis/cell death at later time points (Fig. 1A). Pretreatment with 20 μmol/L zVAD-fmk significantly reduced the amount of Annexin-positive/PI-negative cells, demonstrating a role of caspase-dependent processes.

Jurkat A3 cells were also sensitive to the cytotoxic action of DHA (Fig. 1C and D). Similar to Jurkat E6.1 cells, A3 cells responded to DHA treatment with a time- and concentration-dependent breakdown of $\Delta\Psi_m$, a collapse of the phosphatidylserine asymmetry in the cytoplasmic membrane, the activation of caspases, and nuclear fragmentation indicative of apoptosis (Fig. 1C and D; Supplementary Fig. S2A and B, and data not shown).

DHA was also cytotoxic to primary human transformed cells isolated from the peripheral blood of patients with B-cell CLL. Treatment with 40 μmol/L DHA increased the number of dead cells compared with untreated control cells by 1.7- to 2.3-fold, with additional absolute death rates of ≤15% for five of six patients, to 30% for one of the six patients analyzed. However, as shown by Hoechst 33342/PI and FITC-Annexin/PI staining, DHA treatment mostly induced necrotic cell death (Supplementary Fig. S2C, S2D, and not shown). Malignant B-CLL cells were also resistant to doxorubicin-induced apoptosis, suggesting a general dysfunction of the intrinsic apoptosis pathway (23). Former therapeutic intervention, the loss of a functional ataxia telangiectasia mutated protein, or expression of the cell surface marker CD38 may contribute to apoptosis resistance of B-CLL cells (Supplementary Table S1).

DHA-induced apoptosis in Jurkat cells relies on the intrinsic death pathway

To verify the contribution of the extrinsic pathway, we compared the cytotoxic action of DHA in wild-type, caspase-8 negative, and FADD-negative Jurkat A3 cells. DHA induced apoptosis with almost similar potency in the three cell lines; no prominent differences in the levels of cells with depolarized mitochondria, FITC-Annexin V binding, DNA fragmentation, apoptotic nuclear morphology, or caspase activation were detected (Fig. 1C and D; Supplementary Fig. S2A and B, and data not shown). This shows that caspase-8 and FADD are dispensable for DHA-induced cell death in Jurkat cells. The slightly reduced apoptotic response of caspase-8–negative Jurkat cells may reflect the reduced amplification of the apoptosis signal downstream of the mitochondria through caspase-8 (Fig. 1C). The addition of the pan-caspase inhibitor zVAD-fmk abrogated DHA-induced caspase-3 activation and nuclear fragmentation, demonstrating that caspase activation is required for DHA-induced cell death. However, a low basal level of PARP cleavage was still detectable in the zVAD-fmk–treated samples, particularly in FADD-negative A3 cells (Fig. 1D; Supplementary Fig. S2B). Because the presence of zVAD-fmk also triggered the appearance of necrotic nuclei in

Published OnlineFirst July 27, 2010; DOI: 10.1158/1535-7163.MCT-10-0051

Hoechst 33342/PI–stained samples (Fig. 1D), this residual PARP cleavage may be a result of the induction of necrosis (24–26).

We next analyzed the importance of the intrinsic apoptosis pathway. For this, we used Jurkat A3 cells with Western blot–confirmed expression of a caspase-9 DN mutant (data not shown). The presence of caspase-9 DN largely decreased DHA-induced nuclear fragmentation compared with wild-type cells, suggesting a caspase-9–dependent pathway. However, when ≥20 μmol/L DHA was used, a significant increase in apoptotic death was also observed in caspase-9 DN cells (Fig. 2A and B).

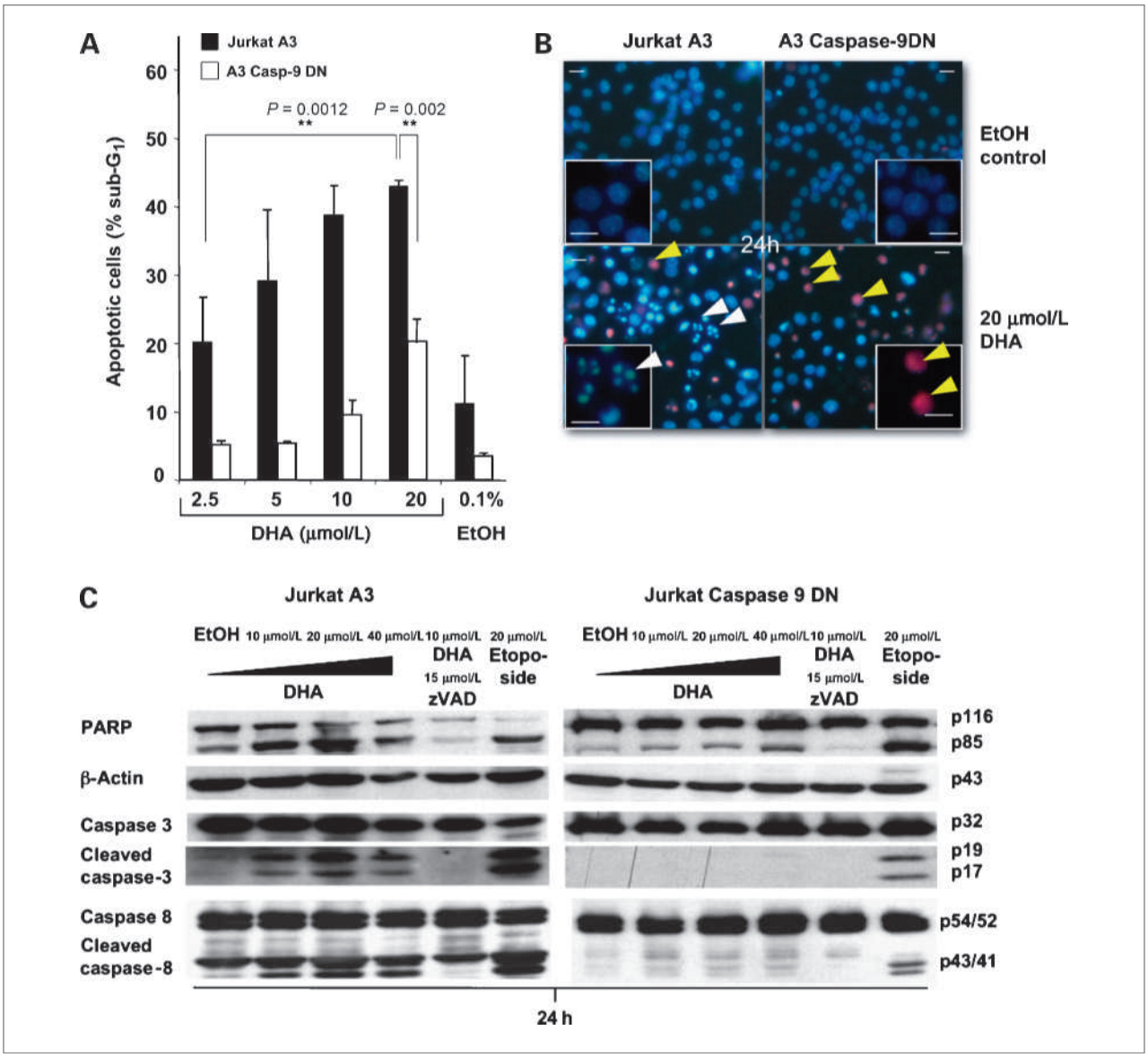

Figure 2. Proapoptotic signaling of DHA involves caspase-9. Jurkat A3 wild-type cells and Jurkat A3 cells expressing a DN mutant of caspase-9 (Jurkat caspase-9 DN) were treated for 24 h with 0 to 40 μmol/L DHA as indicated. Induction of apoptosis was determined by flow cytometry on loading of the cells with PI in a hypotonic citrate buffer and measuring the percentage of cells in sub-G_1 (DNA fragmentation) and fluorescence microscopy (nuclear fragmentation) as described in Fig. 1B. Moreover, we used Western blot analysis to determine caspase activation. Treatment with 0.1% ethanol was used as solvent control. Etoposide, a chemotherapeutic agent known to induce apoptosis via the intrinsic pathway, was used as a control for functional disruption of this pathway. A, DHA treatment induced a concentration-dependent increase in cell numbers with hypodiploid nuclei (sub–G_0-G_1 fraction) indicative of DNA fragmentation in Jurkat A3 cells. The cell fraction in sub–G_0-G_1 was largely reduced in Jurkat caspase-9 DN cells. Data are means ± SD ($n = 3$; ANOVA: *, $P < 0.05$; **, $P < 0.01$; ***, $P < 0.001$; and two tailed P values of paired t tests). B, whereas DHA treatment readily induced apoptosis in Jurkat A3 cells, caspase-9 DN cells displayed mainly necrotic death 24 h after DHA treatment. Data are representative microscopic pictures at 20-fold primary magnification (inset, 40-fold magnification; white scale bars, 10 μm). C, reduced levels of active caspase-3 and caspase-8 as well as cleaved PARP in the presence of caspase-9 DN compared with caspase-9–proficient A3 cells corroborate the importance of caspase-9 for DHA-induced apoptosis. Data are representative Western blots from three similar experiments. Preincubation with 15 μmol/L of the pan-caspase inhibitor zVAD-fmk was used as control for the relevance of caspase-mediated events.

Published OnlineFirst July 27, 2010; DOI: 10.1158/1535-7163.MCT-10-0051

This known phenomenon of incomplete apoptosis inhibition by caspase-9 DN has been attributed to the fact that the caspase-9 DN protein competes with the endogenous caspase-9 for binding sites in the apoptosome and is therefore not able to fully block apoptosis (27). The presence of the caspase-9 DN mutant also prevented the proteolysis of caspase-3 and caspase-8 and largely reduced PARP cleavage (Fig. 2C). Inhibition of caspase-8 processing in caspase-9 DN cells supports the above-mentioned observation that caspase-8 becomes activated downstream of caspase-9 during DHA-induced apoptosis.

Interestingly, 20 and 40 μmol/L DHA triggered a caspase-3–independent PARP cleavage and necrosis in caspase-9 DN cells (Fig. 2B and C). We therefore tested whether DHA may activate a PARP- and AIF-dependent programmed necrosis. In this pathway, AIF is released from the mitochondria in a process that involves proteolysis of full-length AIF to a 57-kDa truncated protein (26, 28). However, treatment of caspase-9 DN Jurkat cells with up to 40 μmol/L DHA did not increase cellular levels of truncated AIF, arguing against a role of programmed necrosis in the caspase-3–independent death of caspase-9 DN Jurkat cells (data not shown).

Role of Bcl-2 proteins in DHA-induced apoptosis

Because antiapoptotic Bcl-2 and Bcl-xL are known to suppress the activation of the intrinsic pathway, we next investigated whether overexpression of these proteins would inhibit DHA-induced apoptosis. DHA induced substantial caspase activation and apoptosis in Jurkat vector cells, an effect that was inhibited by pretreatment with zVAD-fmk. Overexpression of Bcl-2 and Bcl-xL almost completely abrogated DHA-induced breakdown of $\Delta\Psi_m$ and DNA fragmentation, with Bcl-xL being more effective than Bcl-2 (Fig. 3A and B). Similar observations were made when analyzing DHA-induced apoptosis by fluorescence microscopy of Hoechst 33342/PI–stained cells (data not shown). Bcl-2 and Bcl-xL also inhibited DHA-induced caspase activation, although some residual cleavage of caspase-9 and PARP was observed in Jurkat Bcl-2 cells in response to 40 μmol/L DHA (Fig. 3B and data not shown).

To substantiate the role of the intrinsic apoptosis pathway, we next determined the involvement of the two crucial apoptosis effectors, Bax and Bak, in DHA-induced apoptosis. The role of Bak was analyzed using the Bak-proficient JCaM1.6 subline (JCaM Bak pos.) and a Bak-deficient JCaM1.6 subline (JCaM Bak neg.). Because JCaM1.6 cells—like most other Jurkat cells—do not express Bax, Bak-negative JCaM cells are deficient for Bax and Bak (19). Whereas Bak-positive JCaM cells were highly sensitive to DHA-induced breakdown of $\Delta\psi_m$, caspase activation, and apoptosis, Bak-negative JCaM cells were completely resistant to DHA-induced apoptosis (Fig. 4A and B). Only a slight cleavage of PARP without activation of caspase-3 was observed in Bak-negative JCaM cells on treatment with 40 μmol/L DHA. This suggests a caspase-3–independent PARP processing in these apoptosis-resistant cells.

As shown in Fig. 4B and C, Bak-dependent apoptosis in response to DHA was not associated with changes in the expression levels of Bak or Bcl-2 but rather with an activation-associated conformational change of Bak that was detected by flow cytometry using an activation-specific Bak antibody.

To prove the functional relevance of Bak deficiency for resistance to DHA-induced apoptosis, we finally analyzed the sensitivity of Bak-positive JCaM cells to treatment with DHA after silencing of Bak expression using RNAi technology. Forty-eight hours after electroporation with 0.5 to 1.0 μmol/L anti-*bak* siRNA, Bak expression was reduced by 49% compared with untransfected JCaM Bak-positive cells or cells transfected with nontargeted siRNA (Fig. 4D, left). Silencing of Bak resulted in almost complete abrogation of DHA-induced apoptosis in Bak-positive JCaM cells even in the presence of 40 μmol/L DHA.

The role of Bax was analyzed in the HCT116 colon carcinoma cell model using Bax/Bak–positive HCT116 wild-type (wt) cells and a Bax-negative/Bak-positive HCT116 mutant (21). Loss of Bax largely decreased the sensitivity of HCT116 cells to DHA-induced apoptosis, corroborating our findings on the role the intrinsic death pathway in a solid human tumor cell model (Fig. 4A).

In Jurkat cells with low endogenous levels of Bcl-xL and Bcl-2, Bak is kept in check by antiapoptotic Mcl-1 (20). As shown in Fig. 4B and Supplementary Fig. S3, treatment with DHA induced a concentration-dependent loss in Mcl-1 in the Bak-positive JCaM cells, which was only slightly affected by pretreatment of cells with zVAD-fmk. In contrast, Mcl-1 downregulation was not observed in apoptosis-deficient Bak-deficient JCaM cells, suggesting that downregulation of Mcl-1 depends on proper induction of apoptosis.

Interestingly, DHA treatment also induced an increase in the levels of the Mcl-1–interacting BH-3–only protein NOXA. Although the basal levels of NOXA were slightly lower in Bak-positive compared with the Bak-negative JCaM cells, treatment with DHA resulted in a similar increase in the NOXA levels in both cell types (Fig. 4B). Importantly, silencing of NOXA in Bak-positive JCaM cells using 1 μmol/L anti–*noxa* siRNA reduced the NOXA protein levels by ~57%, an effect that was paralleled by a 52% reduction in cells with apoptotic DNA fragmentation after DHA treatment (Fig. 4D, right). These observations strongly support a role of NOXA in the regulation of DHA-induced apoptosis. Because the loss of Bak and treatment with zVAD-fmk did not prevent the upregulation of NOXA, it is tempting to speculate that NOXA-upregulation occurs upstream of Bak activation.

Apoptosis induction by DHA involves ROS generation

We were then interested in the events initiating DHA-induced apoptosis upstream of Bak (29). For this, the

Published OnlineFirst July 27, 2010; DOI: 10.1158/1535-7163.MCT-10-0051

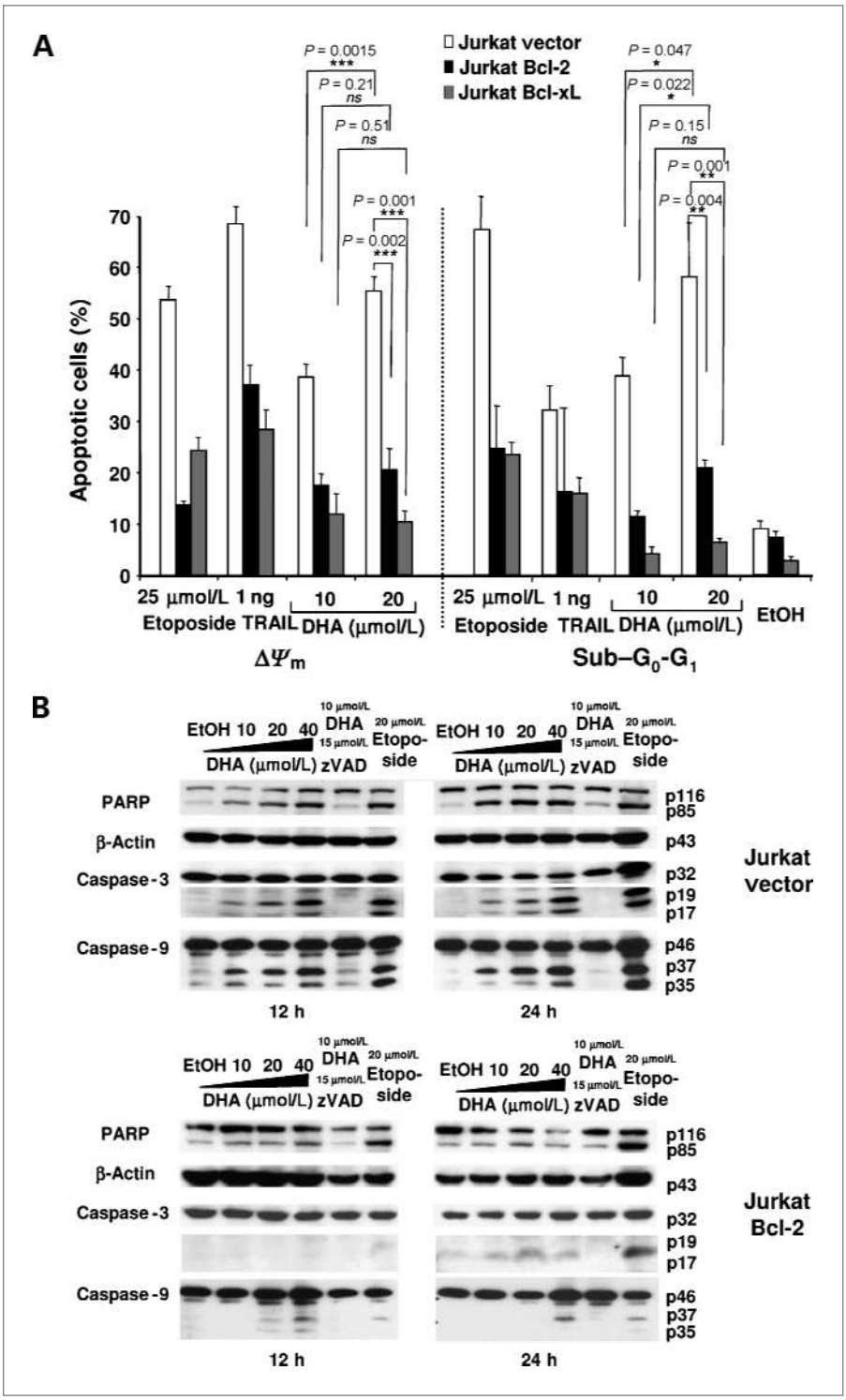

Figure 3. Antiapoptotic Bcl-2 family members interfere with apoptosis induction after DHA treatment. Jurkat vector cells and Jurkat cells with constitutive overexpression of Bcl-2 or Bcl-xL were treated for 24 h with 0 to 40 μmol/L DHA as indicated. Treatment with 0.1% ethanol was used as solvent control. Etoposide (20 or 25 μmol/L) or TRAIL (1 ng/mL) were used to show disruption of the intrinsic and integrity of the extrinsic apoptosis pathway, respectively. Overexpression of Bcl-2 or Bcl-xL conferred prominent protection against DHA-induced apoptosis. A, quantification of apoptosis by flow cytometry (breakdown of $\Delta\psi_m$, DNA fragmentation) as described in Fig. 1C. Data are specific values normalized on the solvent (ethanol) control: % treated cells − % untreated cells (means ± SD; $n = 3$). Significant differences were verified by ANOVA (*, $P < 0.05$; **, $P < 0.01$; ***, $P < 0.001$) and paired t tests. B, levels of active caspase-3 and caspase-9 as well as cleaved PARP were determined by Western blot analysis. Data are representative results from three similar experiments.

generation of ROS was measured in DHA-treated Bak-positive and Bak-negative JCaM cells by flow cytometry using the hydrogen peroxide–induced ROS-sensitive fluorescent dye DCFDA. DHA induced a significant ROS production in Bak-positive and Bak-negative JCaM cells (Fig. 5A). The ROS levels triggered by DHA treatment were comparable with those measured on addition of 250 μmol/L H_2O_2, which served as a positive control. Interestingly, ROS production by DHA was almost similar in Bak-positive and Bak-negative cells and was not inhibited by the addition of zVAD-fmk, suggesting their generation upstream of the mitochondria. To corroborate

Published OnlineFirst July 27, 2010; DOI: 10.1158/1535-7163.MCT-10-0051

our findings, we performed an additional set of experiments in Jurkat E6.1 cells using the superoxide-sensitive dye dihydroethidium. DHA treatment also increased the intracellular superoxide levels in a concentration-dependent manner (Supplementary Fig. S4A). ROS production was significantly reduced if cells were incubated with the radical scavengers *N*-acetylcysteine or glutathione before DHA treatment (Fig. 5A; Supplementary

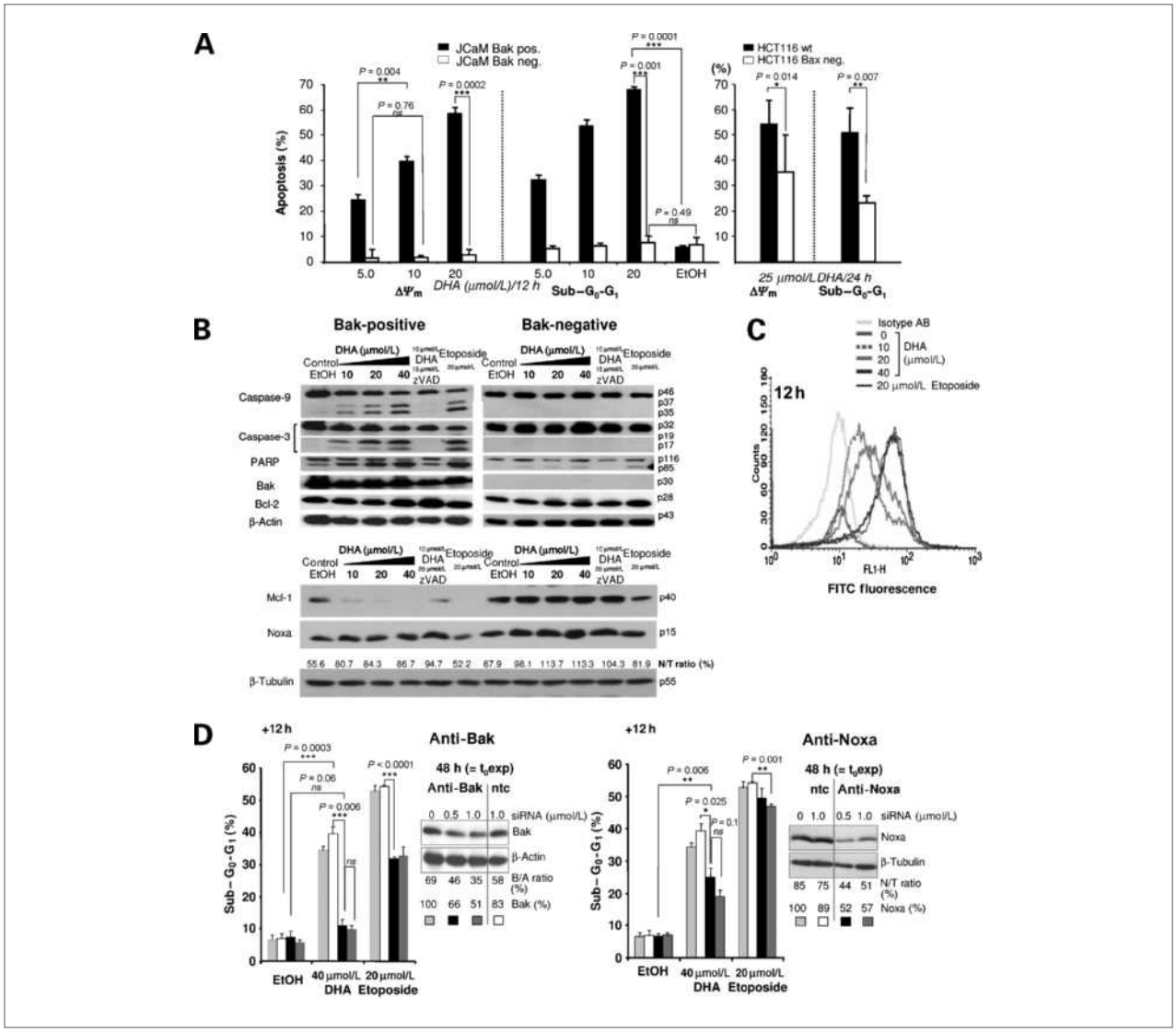

Figure 4. DHA-induced apoptosis depends on the expression of proapoptotic multidomain Bcl-2 effector proteins. Bak-positive and Bak-negative JCaM cells as well as Bax-positive/Bak-positive (wt) and Bax-negative/Bak-positive HCT116 cells were treated for 12 h (JCaM cells) or 24 h (HCT116 cells) with 0 to 40 μmol/L DHA as indicated. Induction of apoptosis was determined by flow cytometry (A), analyzing breakdown of the mitochondrial membrane potential ($\Delta\psi_m$); DNA fragmentation (sub-G_1 peak); and Western blot analysis (B; caspase activation). Treatment with 0.1% ethanol was used as solvent control. A, loss of Bak abrogated DHA-induced apoptosis in JCaM cells, and loss of Bax decreased DHA-induced apoptosis in HCT116 colon carcinoma cells. Data are specific values normalized by subtraction of the solvent control, % treated cells − % untreated cells, from three independent experiments (means ± SD). The significance of the results was tested by ANOVA (*, $P < 0.05$; **, $P < 0.01$; ***, $P < 0.001$; ns, not significant) and two-tailed *P* values of paired *t* tests. B, DHA treatment leads to caspase activation and Mcl-1 downregulation in a Bak-dependent manner. Data are representative Western blots of full-length and cleaved caspase-3, caspase-8, and PARP as well as expression of the Bcl-2 family proteins Bak, NOXA, Bcl-2, and Mcl-1. Etoposide (20 μmol/L) was used as a control for the disruption of the intrinsic pathway. Relative intensities of NOXA compared with tubulin expression were calculated from the ratio of the mean densities of the probe, and the control signal in percent (N/T ratio = mean value NOXA/mean value α/β-tubulin × 100%). C, treatment with DHA induced activation of Bak. Activation-specific conformational changes of Bak were determined 12 h after treatment with 0 to 40 μmol/L DHA by flow cytometry in paraformaldehyde-fixed Bak-positive JCaM cells using an activation-specific mouse monoclonal anti-Bak antibody (A03) and an Alexa Fluor488–conjugated goat anti-mouse secondary antibody, respectively. Data from one representative of three similar experiments are shown. D, RNAi-mediated silencing of *bak* (left) or *noxa* (right) expression largely reduced DHA-induced apoptosis. Apoptosis was quantified by flow cytometric determination of hypodiploid nuclei 12 h after treatment with 40 μmol/L DHA. Treatment experiments started 48 h after siRNA transfection when silencing efficacies of 51% (Bak) or of 57% (NOXA) at the protein level were obtained. Data are means ± SD ($n = 3$).

Published OnlineFirst July 27, 2010; DOI: 10.1158/1535-7163.MCT-10-0051

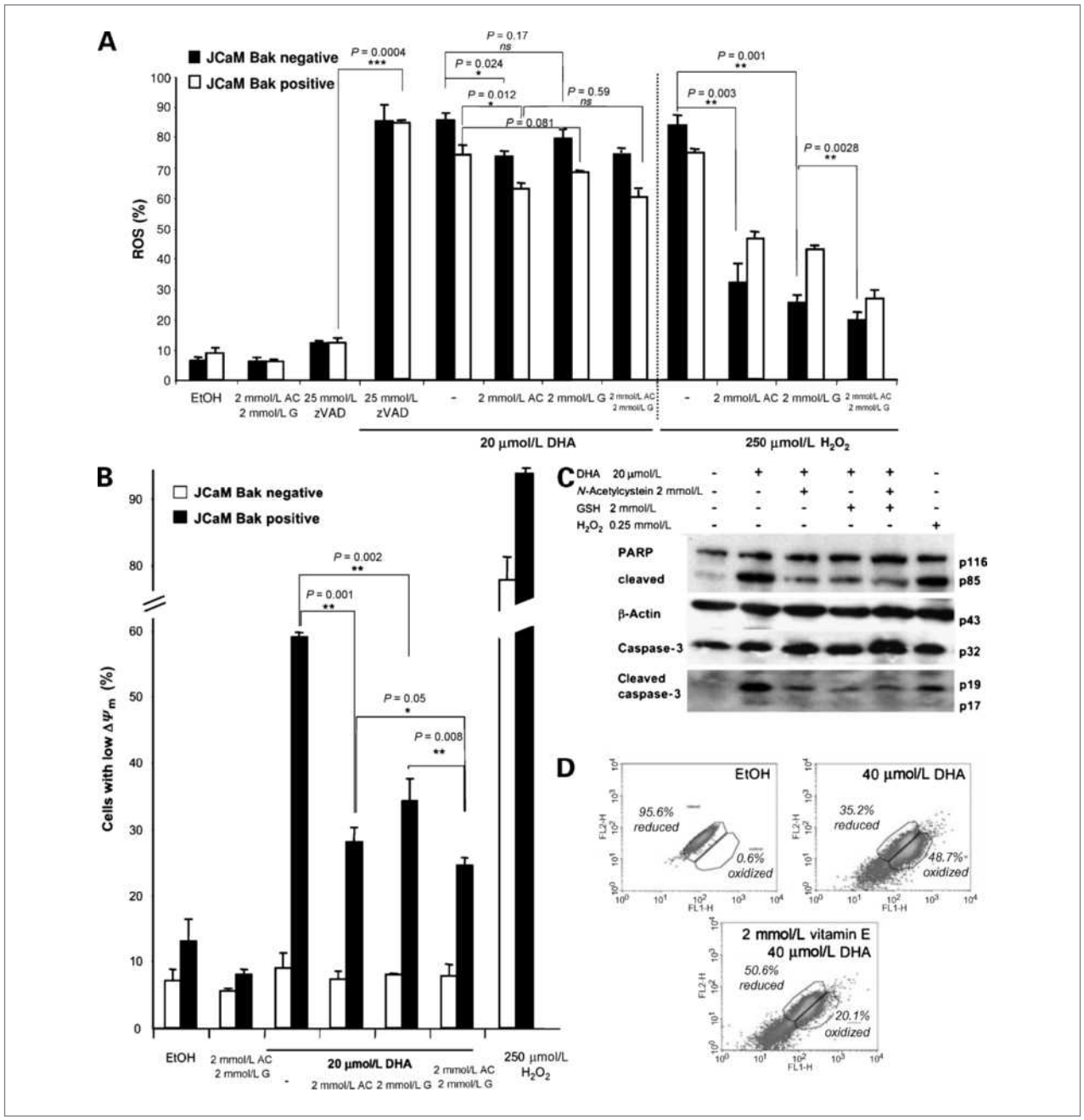

Figure 5. Intracellular apoptosis signaling by DHA is partially dependent on ROS. A, DHA treatment induces the formation of intracellular ROS that can be inhibited to some extent by preincubation with radical scavengers. Jurkat E6.1 cells were preincubated for 30 min in the absence or presence of the radical scavengers *N*-acetylcysteine (AC, 2 mmol/L) and/or glutathione (G, 2 mmol/L) and then treated for 12 h with 20 µmol/L DHA. ROS formation was determined on loading of the cells with the oxidation-sensitive dye DCFDA. Treatment with 250 µmol/L H_2O_2 served as positive control for ROS (means ± SD, $n = 3$; ANOVA: *, $P < 0.05$; **, $P < 0.01$; ***, $P < 0.001$; and two tailed P values of paired t tests). B, the presence of radical scavengers reduced DHA-induced apoptosis. Jurkat E6.1 cells were treated with 20 µmol/L DHA for 12 h without or with prior incubation with *N*-acetylcysteine or glutathione as indicated. Apoptosis levels were quantified 12 h after addition of DHA by flow cytometry, analyzing breakdown of $\Delta\psi_m$ (TMRE staining). Data are means ± SD ($n = 3$); analysis of statistical significance was done by ANOVA (*, $P < 0.05$; **, $P < 0.01$; ***, $P < 0.001$); and two tailed P values of paired t tests are given. C, the presence of radical scavengers reduced DHA-induced caspase activation. Jurkat E6.1 cells were treated with 20 µmol/L DHA for 12 h without or with prior incubation with 2 mmol/L *N*-acetylcysteine or glutathione. Activation of caspase-3 and cleavage of the caspase-3 substrate PARP were analyzed by Western blotting. Data are representative blots. D, DHA induces oxidation of membrane compounds, which can be partially prevented by preincubation with the lipophilic radical scavenger vitamin E. Jurkat E6.1 cells were preincubated for 30 min with or without 2 mmol/L vitamin E, and then treated with 40 µmol/L DHA as indicated. ROS formation was determined on loading of the cells with the membrane-targeted fluorescent dye Bodipy 12 h after treatment. The decrease in green fluorescence (x axis = Fl-1) together with the increase in red fluorescence (y axis = Fl-2) of Bodipy is indicative of membrane oxidation. Data are representative results from three similar experiments.

Published OnlineFirst July 27, 2010; DOI: 10.1158/1535-7163.MCT-10-0051

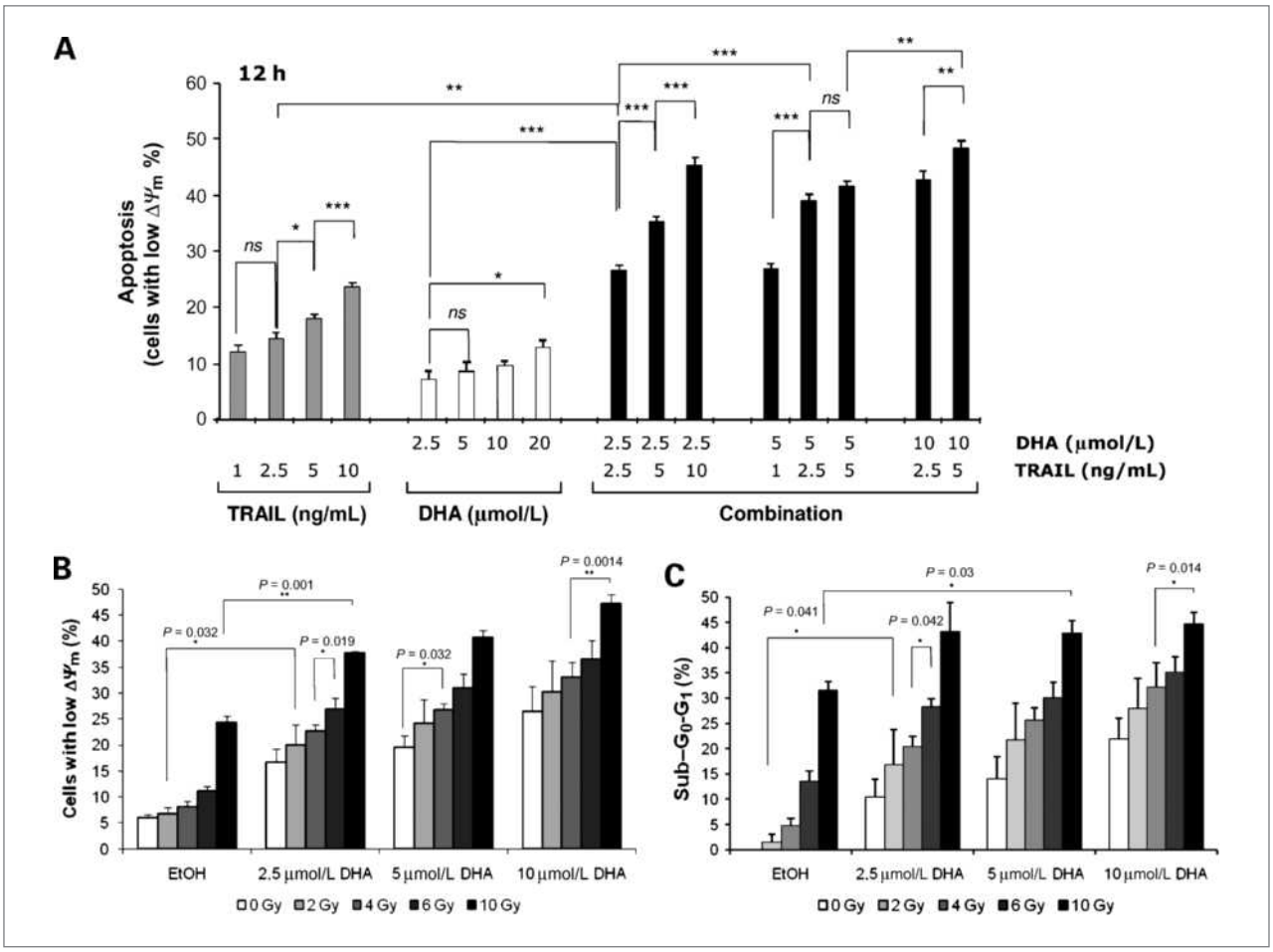

Figure 6. Addition of DHA increases the proapoptotic action of TRAIL and radiotherapy. Combined treatment with DHA and TRAIL or radiotherapy increased apoptosis levels compared with the single treatments. A, Jurkat E6.1 cells were treated for 12 h with 0, 2.5, 5, 10, or 20 μmol/L DHA; 0, 1, 2.5, 5, or 10 ng/mL human recombinant TRAIL; or submitted to combined treatment as indicated. For combination treatment, TRAIL was added 10 min before addition of DHA. Breakdown of $\Delta\Psi_m$ on treatment with TRAIL or DHA alone or in combination was measured by flow cytometry as described in Fig. 1. B and C, Bak-positive Jurkat cells were treated for 12 h with 0, 2.5, or 10 μmol/L DHA; irradiated with 0, 2, 4, 6, or 10 Gy; or submitted to combination treatment as indicated. In the combination experiments, DHA was added 10 min before irradiation. Breakdown of $\Delta\Psi_m$ (B) and apoptotic DNA fragmentation (C; sub-G_1) were determined by flow cytometry as described in Fig. 1C and Fig. 2A, respectively. Data are means ± SD ($n = 3$; ANOVA: *, $P < 0.05$; **, $P < 0.01$; ***, $P < 0.001$; and two-tailed P values of paired t tests).

Fig. S4A). The reduction of ROS production by these radical scavengers resulted in a significant reduction in the DHA-induced collapse of $\Delta\Psi_m$, caspase activation, and apoptosis, although a combination of both compounds did not result in a further prominent increase in the protective effects (Fig. 5B and C; Supplementary Fig. S4B).

To gain insight into putative cellular targets of the ROS, we used the membrane-targeted ROS-sensitive dye Bodipy. This dye indicates increased levels of ROS in cellular membranes through an oxidation-triggered fluorescence shift. As shown in Fig. 5D, treatment with 40 μmol/L DHA induced an increased fluorescence intensity of Bodipy in FL-1 (x axis), which was accompanied by a decreased fluorescence in Fl-2 (y axis), characteristic for oxidation of the dye by increased membrane ROS levels. This effect could, at least partially, be reversed by the addition of membrane-targeted ROS scavenger vitamin E before DHA treatment (Fig. 5D). These data suggest that increased oxidation of proteins or lipids located in cellular membranes may contribute to the cytotoxic action of DHA.

DHA improves the proapoptotic action of TRAIL and irradiation

After defining the molecular details of DHA-induced apoptosis, we analyzed the potential of DHA to increase the efficacy of standard (radiotherapy) or targeted (TRAIL) anticancer therapies. Isobologram analysis was used to test the additive or synergistic effects of the combination treatments (22). Combining 2.5 to 5 μmol/L DHA and 2.5 to 5 ng/mL TRAIL increased apoptosis of Jurkat E6.1 cells in a synergistic manner (Fig. 6A; Supplementary Table S2). In contrast, in the presence of 10 ng TRAIL or 10 μmol/L DHA, the combination effects were

Published OnlineFirst July 27, 2010; DOI: 10.1158/1535-7163.MCT-10-0051

only additive. The cytotoxicity of low-dose radiotherapy (2 and 4 Gy) was also increased in a synergistic manner by the addition of low DHA concentrations, whereas the addition of 10 μmol/L DHA yielded only additive combination effects (Fig. 6C; Supplementary Table S2). Using irradiation with 10 Gy, the combination effects were always less than additive. Our findings suggest a potential benefit when combining DHA with stimuli of the extrinsic or the intrinsic pathway, respectively. It is tempting to speculate that DHA-mediated formation of ROS may contribute to the observed effects.

Discussion

Recent studies suggest a potential use of artemisinin and its active metabolite DHA as anticancer agents (6, 30–32). However, the molecular details of DHA-induced apoptosis remain unclear. Here, we show that DHA induces apoptosis in Jurkat T-lymphoma cells via the intrinsic apoptosis pathway. Moreover, we show for the first time a crucial role of Bak for DHA-induced apoptosis in these cells.

Although a recent report already showed activation of caspase-3 and mitochondrial changes in response to DHA treatment (33), our investigations provide a more profound insight into apoptosis regulation by DHA: We show that the proapoptotic action of DHA requires the sequential activation of caspase-9 and caspase-3 without a need for critical components of the extrinsic apoptosis pathway, namely caspase-8 or FADD. The observations that overexpression of the antiapoptotic proteins Bcl-2 and Bcl-xL abrogate DHA-induced apoptosis and that activation of caspase-8 occurs only as a secondary event downstream of the mitochondria further corroborate our assumption about the strict dependence of DHA-induced apoptosis from activation of the intrinsic pathway.

Even more important, our data emphasize a prominent role of proapoptotic multidomain Bcl-2 proteins for the regulation of DHA-induced apoptosis: Loss of Bak or reduction of Bak expression by RNAi led to complete abrogation of DHA-induced caspase activation and apoptosis in Bax-deficient Jurkat cells. This supports earlier observations on the broad resistance of Bax/Bak–deficient cells to stimuli of the intrinsic apoptosis pathway. Interestingly, loss of Bax significantly reduced cellular sensitivity of HCT116 colon carcinoma cell line to DHA-induced apoptosis. Because earlier investigations showed a functional redundancy of Bax and Bak in stress-induced apoptosis, we speculate that in Bax-deficient HCT116 cells, Bak may replace Bax to execute DHA-induced apoptosis. However, it cannot be excluded that similar to some other death stimuli, DHA may preferentially depend on either Bax or Bak for the execution of apoptosis in particular cell systems (34).

Thus, the signaling pathway of DHA-induced apoptosis mimics that of chemotherapy and radiotherapy, which similarly induce apoptosis mainly via the intrinsic pathway (35, 36).

Whereas the intracellular levels of endogenous Bak and Bcl-2 remained rather unchanged, DHA treatment resulted in an activation-associated change in the conformation of Bak and a rapid decrease in the levels of antiapoptotic Mcl-1. This is in contrast to findings obtained in human ovarian cancer cell lines in which DHA-induced apoptosis was accompanied by an increase of Bax and Bad and a decrease of Bcl-xL and Bcl-2 (11). Also, in murine endothelial cells, *bcl-2* and *bax* were inversely regulated by DHA at the transcriptional level (12, 37). Moreover, treatment of mice bearing xenograft tumors with DHA reduced Bcl-2 levels (38, 39). These discrepancies may be due to the differences in the dependence of distinct cellular systems on specific proapoptotic and antiapoptotic Bcl-2 family members for mitochondrial homeostasis and apoptosis (17, 18).

In this regard, Bax-deficient Jurkat cells seem to be entirely dependent on Mcl-1 (20, 40, 41). The prominent inhibitory action of Bcl-xL and the downregulation of Mcl-1 during DHA-induced apoptosis fit well into the concept that proapoptotic Bak is kept in check by Mcl-1 and Bcl-xL and that apoptosis execution requires abrogation of the inhibitory action of these antiapoptotic Bcl-2 family members (42, 43).

In parallel with the decrease in full-length Mcl-1, we observed an increase of the BH-3–only protein NOXA, a suggested antagonist of Mcl-1 (44). Because RNAi-mediated downregulation of NOXA inhibited DHA-induced apoptosis to some extent, a role of NOXA in DHA-mediated apoptosis can be assumed. This is reminiscent of the role of NOXA and Mcl-1 in the cellular response to the nonsteroidal anti-inflammatory drug celecoxib, histone deacetylase inhibitors, and proteasome inhibitors (20, 45). Although the observations that loss of Bak and pretreatment with zVAD-fmk do not prevent the upregulation of NOXA suggest that NOXA upregulation is an upstream event, the exact role of NOXA in DHA-induced apoptosis remains to be defined.

Altogether, these data suggest that DHA potently induces apoptosis in apoptosis-competent cells, whereas in apoptosis-resistant cells, such as primary transformed cells isolated from B-CLL patients or cells with deficiency in proteins of the core apoptotic machinery, DHA triggers a caspase-independent necrotic cell death. The failure of DHA to induce an increase in the cellular levels of truncated AIF in necrosis-sensitive Jurkat caspase-9 DN cells argues against a role of the PARP/AIF pathway for DHA-induced necrosis (26, 28). The molecular details of DHA-induced necrotic cell death warrant further investigation.

DHA-induced mitochondrial alterations and apoptosis were inhibited by pretreatment with the radical scavengers *N*-acetylcysteine and reduced glutathione, suggesting that the generation of ROS is a characteristic hallmark of DHA-induced cell death. This corroborates recent observations obtained by Efferth and colleagues using the DHA-related drug artesunate (13). However, here, we show in addition that inhibition of ROS by radical scavengers is almost

Published OnlineFirst July 27, 2010; DOI: 10.1158/1535-7163.MCT-10-0051

independent from Bak, suggesting that ROS formation occurs upstream of the mitochondria. Importantly, using a membrane-specific ROS-sensitive dye, we show for the first time that DHA increases the oxidation of membrane compounds in tumor cells. This observation is reminiscent of artemisinin-induced oxidative membrane damage in *P. falciparum* (4). However, the induction of oxidative membrane damage is a completely novel facet of the antineoplastic DHA action that up to now had solely been attributed to DNA damage (46).

Based on our improved knowledge on the molecular determinants of DHA-induced apoptosis, we were able to define promising partners for combined treatment strategies. At first, the combination of DHA with recombinant human TRAIL, a known stimulus of the extrinsic apoptosis pathway, increased death rates compared with single-drug treatment in a synergistic manner, at least in the low-dose range. This is of particular interest because TRAIL is known to induce apoptosis even in cells with resistance to stimuli of the intrinsic pathway or under conditions that impair the action of standard chemotherapy or radiotherapy (47).

Moreover, the combination of low-dose irradiation and DHA treatment resulted in a dose-dependent additive to synergistic increase in apoptotic cell death. These findings corroborate recent *in vitro* data on increased efficacy of DHA in Molt-4 and glioma cells when combined with irradiation (48). Further reports from other laboratories showed beneficial effects of DHA on the cytotoxic action of sodium butyrate (49), doxorubicin (13), gemcitabine (50), temozolomide (51), carboplatin (13, 38), and cyclophosphamide (52), respectively. Thus, a sensitizing effect of DHA can even be achieved in combination with other stimuli of the intrinsic apoptosis pathway.

On the one hand, the radical-forming potency of DHA may facilitate or enhance chemotherapy- and radiotherapy-induced DNA damage and thus apoptosis. On the other hand, DHA may decrease the cellular death threshold and thus increase cellular sensitivity to apoptosis induction by inhibiting survival-promoting apoptosis regulators. As an example, by inhibiting the transcription factor NF-κB, DHA would prevent NF-κB–mediated upregulation of antiapoptotic Bcl-2, Bcl-xL, and/or survivin (53). Inhibition of NF-κB signaling may be of particular importance for the cellular response to DHA under conditions that trigger activation of NF-κB such as inflammation or ionizing radiation (15).

In contrast to apoptosis-competent Jurkat T-lymphoma cells, malignant cells isolated from B-CLL patients were resistant to DHA-induced apoptosis and mostly underwent necrotic cell death on DHA treatment. Because these cells were also resistant to doxorubicin-induced apoptosis, a more general resistance of the cells to stimuli of the intrinsic apoptosis pathway can be assumed. It will be important to identify the cellular factors that determine resistance to apoptosis and sensitivity to necrosis in these primary cells to define biomarkers for the selection of responsive patients.

In summary, DHA, artemisinin, and related compounds are promising antineoplastic agents with a particular molecular mechanism of action. The use of artesunate, DHA, and related compounds in anticancer treatment is of particular interest because the broad use of these compounds in antimalaria treatment has shown low toxicity at least during short-term treatment (up to 7 days) with individual doses of up to 1 g per day (54). Further investigations are needed to analyze the molecular details of the interaction of DHA with chemotherapy or radiotherapy, and to test whether the combination effects of DHA can be confirmed in xenograft tumors in the mouse.

Disclosure of Potential Conflicts of Interest

No potential conflicts of interest were disclosed.

Acknowledgments

We thank P. Juo and J. Blenis (Boston, MA) for the caspase-8 and FADD-negative Jurkat cells, B. Leber (Hamilton, Ontario, Canada) for the generous gift of the Bcl-2 vectors, E. Alnemri (Philadelphia, PA) for the caspase-9 DN construct, B. Vogelstein (Johns Hopkins, Baltimore, MD) and P.T. Daniel (Department of Hematology, Oncology and Tumor Immunology, University Medical Center Charité, Campus Berlin-Buch, Humboldt University, Berlin, Germany) for the HCT116 wild-type and Bax-deficient HCT116 cells, and Michael Möllmann for excellent technical support.

The costs of publication of this article were defrayed in part by the payment of page charges. This article must therefore be hereby marked *advertisement* in accordance with 18 U.S.C. Section 1734 solely to indicate this fact.

Received 01/21/2010; revised 07/17/2010; accepted 07/20/2010; published OnlineFirst 07/27/2010.

References

1. Klayman DL. Qinghaosu (artemisinin): an antimalarial drug from China. Science 1985;228:1049–55.
2. Meshnick SR, Taylor TE, Kamchonwongpaisan S. Artemisinin and the antimalarial endoperoxides: from herbal remedy to targeted chemotherapy. Microbiol Rev 1996;60:301–15.
3. Eckstein-Ludwig U, Webb RJ, Van Goethem ID, et al. Artemisinins target the SERCA of *Plasmodium falciparum*. Nature 2003;424:957–61.
4. O'Neill PM, Posner GH. A medicinal chemistry perspective on artemisinin and related endoperoxides. J Med Chem 2004;47:2945–64.
5. Meshnick SR. Artemisinin: mechanisms of action, resistance and toxicity. Int J Parasitol 2002;32:1655–60.
6. Efferth T. Molecular pharmacology and pharmacogenomics of artemisinin and its derivatives in cancer cells. Curr Drug Targets 2006;7:407–21.
7. Butler AR, Gilbert BC, Hulme P, Irvine LR, Renton L, Whitwood AC. EPR evidence for the involvement of free radicals in the iron-catalysed decomposition of qinghaosu (artemisinin) and some derivatives; antimalarial action of some polycyclic endoperoxides. Free Radic Res 1998;28:471–6.
8. Efferth T, Benakis A, Romero MR, et al. Enhancement of cytotoxicity

Published OnlineFirst July 27, 2010; DOI: 10.1158/1535-7163.MCT-10-0051

of artemisinins toward cancer cells by ferrous iron. Free Radic Biol Med 2004;37:998–1009.
9. Moore JC, Lai H, Li JR, et al. Oral administration of dihydroartemisinin and ferrous sulfate retarded implanted fibrosarcoma growth in the rat. Cancer Lett 1995;98:83–7.
10. Lai H, Sasaki T, Singh NP. Targeted treatment of cancer with artemisinin and artemisinin-tagged iron-carrying compounds. Expert Opin Ther Targets 2005;9:995–1007.
11. Jiao Y, Ge CM, Meng QH, Cao JP, Tong J, Fan SJ. Dihydroartemisinin is an inhibitor of ovarian cancer cell growth. Acta Pharmacol Sin 2007;28:1045–56.
12. Wang Z, Qiu J, Guo TB, et al. Anti-inflammatory properties and regulatory mechanism of a novel derivative of artemisinin in experimental autoimmune encephalomyelitis. J Immunol 2007;179:5958–65.
13. Efferth T, Giaisi M, Merling A, Krammer PH, Li-Weber M. Artesunate induces ROS-mediated apoptosis in doxorubicin-resistant T leukemia cells. PLoS One 2007;2:e693.
14. Ishibashi M, Ohtsuki T. Studies on search for bioactive natural products targeting TRAIL signaling leading to tumor cell apoptosis. Med Res Rev 2008;28:688–714.
15. Suvannasankha A, Crean CD, Shanmugam R, et al. Antimyeloma effects of a sesquiterpene lactone parthenolide. Clin Cancer Res 2008; 14:1814–22.
16. Ashkenazi A. Directing cancer cells to self-destruct with pro-apoptotic receptor agonists. Nat Rev Drug Discov 2008;7:1001–12.
17. Youle RJ, Strasser A. The BCL-2 protein family: opposing activities that mediate cell death. Nat Rev Mol Cell Biol 2008;9:47–59.
18. Brenner D, Mak TW. Mitochondrial cell death effectors. Curr Opin Cell Biol 2009;21:871–7.
19. Rudner J, Mueller AC, Matzner N, et al. The additional loss of Bak and not the lack of the protein tyrosine kinase p56/Lck in one JCaM1.6 subclone caused pronounced apoptosis resistance in response to stimuli of the intrinsic pathway. Apoptosis 2009;14:711–20.
20. Rudner J, Elsaesser SJ, Muller AC, Belka C, Jendrossek V. Differential effects of anti-apoptotic Bcl-2 family members Mcl-1, Bcl-2, and Bcl-xL on celecoxib-induced apoptosis. Biochem Pharmacol 2010; 79:10–20.
21. Zhang L, Yu J, Park BH, Kinzler KW, Vogelstein B. Role of BAX in the apoptotic response to anticancer agents. Science 2000;290:989–92.
22. Berenbaum MC. A method for testing for synergy with any number of agents. J Infect Dis 1978;137:122–30.
23. Svirnovski AI, Shman TV, Serhiyenka TF, Savitski VP, Smolnikova V V, Fedasenka UU. ABCB1 and ABCG2 proteins, their functional activity and gene expression in concert with drug sensitivity of leukemia cells. Hematology 2009;14:204–12.
24. Shah GM, Shah RG, Poirier GG. Different cleavage pattern for poly (ADP-ribose) polymerase during necrosis and apoptosis in HL-60 cells. Biochem Biophys Res Commun 1996;229:838–44.
25. Casiano CA, Ochs RL, Tan EM. Distinct cleavage products of nuclear proteins in apoptosis and necrosis revealed by autoantibody probes. Cell Death Differ 1998;5:183–90.
26. Gobeil S, Boucher CC, Nadeau D, Poirier GG. Characterization of the necrotic cleavage of poly(ADP-ribose) polymerase (PARP-1): implication of lysosomal proteases. Cell Death Differ 2001;8:588–94.
27. Wu GS, Ding Z. Caspase 9 is required for p53-dependent apoptosis and chemosensitivity in a human ovarian cancer cell line. Oncogene 2002;21:1–8.
28. Yu SW, Wang H, Poitras MF, et al. Mediation of poly(ADP-ribose) polymerase-1-dependent cell death by apoptosis-inducing factor. Science 2002;297:259–63.
29. Rosenthal PJ, Meshnick SR. Hemoglobin catabolism and iron utilization by malaria parasites. Mol Biochem Parasitol 1996;83:131–9.
30. Haynes RK, Ho WY, Chan HW, et al. Highly antimalaria-active artemisinin derivatives: biological activity does not correlate with chemical reactivity. Angew Chem Int Ed Engl 2004;43:1381–5.
31. Efferth T, Briehl MM, Tome ME. Role of antioxidant genes for the activity of artesunate against tumor cells. Int J Oncol 2003;23:1231–5.
32. Efferth T, Sauerbrey A, Olbrich A, et al. Molecular modes of action of artesunate in tumor cell lines. Mol Pharmacol 2003;64:382–94.
33. Lu YY, Chen TS, Qu JL, Pan WL, Sun L, Wei XB. Dihydroartemisinin (DHA) induces caspase-3-dependent apoptosis in human lung adenocarcinoma ASTC-a-1 cells. J Biomed Sci 2009;16:16.
34. Reed JC. Proapoptotic multidomain Bcl-2/Bax-family proteins: mechanisms, physiological roles, and therapeutic opportunities. Cell Death Differ 2006;13:1378–86.
35. Li M, Jung A, Ganswindt U, et al. Aurora kinase inhibitor ZM447439 induces apoptosis via mitochondrial pathways. Biochem Pharmacol 2010;79:122–9.
36. Handrick R, Ganswindt U, Faltin H, et al. Combined action of celecoxib and ionizing radiation in prostate cancer cells is independent of pro-apoptotic Bax. Radiother Oncol 2009;90:413–21.
37. Efferth T, Oesch F. Oxidative stress response of tumor cells: microarray-based comparison between artemisinins and anthracyclines. Biochem Pharmacol 2004;68:3–10.
38. Chen T, Li M, Zhang R, Wang H. Dihydroartemisinin induces apoptosis and sensitizes human ovarian cancer cells to carboplatin therapy. J Cell Mol Med 2009;13:1358–70.
39. Chen H, Sun B, Pan SH, et al. Study on anticancer effect of dihydroartemisinin on pancreatic cancer. Zhonghua Wai Ke Za Zhi 2009;47:1002–5.
40. Sinha-Datta U, Taylor JM, Brown M, Nicot C. Celecoxib disrupts the canonical apoptotic network in HTLV-I cells through activation of Bax and inhibition of PKB/Akt. Apoptosis 2008;13:33–40.
41. Dai H, Meng XW, Lee SH, Schneider PA, Kaufmann SH. Context-dependent Bcl-2/Bak interactions regulate lymphoid cell apoptosis. J Biol Chem 2009;284:18311–22.
42. Chen L, Willis SN, Wei A, et al. Differential targeting of prosurvival Bcl-2 proteins by their BH3-only ligands allows complementary apoptotic function. Mol Cell 2005;17:393–403.
43. Certo M, Del Gaizo Moore V, Nishino M, et al. Mitochondria primed by death signals determine cellular addiction to antiapoptotic BCL-2 family members. Cancer Cell 2006;9:351–65.
44. Czabotar PE, Lee EF, van Delft MF, et al. Structural insights into the degradation of Mcl-1 induced by BH3 domains. Proc Natl Acad Sci U S A 2007;104:6217–22.
45. Inoue S, Walewska R, Dyer MJ, Cohen GM. Downregulation of Mcl-1 potentiates HDACi-mediated apoptosis in leukemic cells. Leukemia 2008;22:819–25.
46. Li PC, Lam E, Roos WP, Zdzienicka MZ, Kaina B, Efferth T. Artesunate derived from traditional Chinese medicine induces DNA damage and repair. Cancer Res 2008;68:4347–51.
47. Weinmann M, Marini P, Jendrossek V, et al. Influence of hypoxia on TRAIL-induced apoptosis in tumor cells. Int J Radiat Oncol Biol Phys 2004;58:386–96.
48. Kim SJ, Kim MS, Lee JW, et al. Dihydroartemisinin enhances radiosensitivity of human glioma cells *in vitro*. J Cancer Res Clin Oncol 2006;132:129–35.
49. Singh NP, Lai HC. Synergistic cytotoxicity of artemisinin and sodium butyrate on human cancer cells. Anticancer Res 2005;25: 4325–31.
50. Hou J, Wang D, Zhang R, Wang H. Experimental therapy of hepatoma with artemisinin and its derivatives: *in vitro* and *in vivo* activity, chemosensitization, and mechanisms of action. Clin Cancer Res 2008;14:5519–30.
51. Huang XJ, Li CT, Zhang WP, Lu YB, Fang SH, Wei EQ. Dihydroartemisinin potentiates the cytotoxic effect of temozolomide in rat C6 glioma cells. Pharmacology 2008;82:1–9.
52. Zhou HJ, Zhang JL, Li A, Wang Z, Lou XE. Dihydroartemisinin improves the efficiency of chemotherapeutics in lung carcinomas *in vivo* and inhibits murine Lewis lung carcinoma cell line growth *in vitro*. Cancer Chemother Pharmacol 2010;66:21–9.
53. Chen H, Sun B, Wang S, et al. Growth inhibitory effects of dihydroartemisinin on pancreatic cancer cells: involvement of cell cycle arrest and inactivation of nuclear factor-κB. J Cancer Res Clin Oncol 2010; 136:897–903.
54. White NJ, Ashley EA, Nosten F. Toxic brainstem encephalopathy after artemisinin treatment for breast cancer. Ann Neurol 2006;59: 725–6.

AACR American Association for Cancer Research

Molecular Cancer Therapeutics

Dihydroartemisinin Induces Apoptosis by a Bak-Dependent Intrinsic Pathway

René Handrick, Teona Ontikatze, Kerstin-Daniela Bauer, et al.

Mol Cancer Ther 2010;9:2497-2510. Published OnlineFirst July 27, 2010.